

A novel series of imidazo[1,2-*a*]pyridine derivatives as HIF-1 α prolyl hydroxylase inhibitors

Namal C. Warshakoon,* Shengde Wu, Angelique Boyer, Richard Kawamoto, Justin Sheville, Sean Renock, Kevin Xu, Matthew Pokross, Artem G. Evdokimov, Richard Walter and Marlene Mekel

Procter & Gamble Pharmaceuticals, Inc., 8700 Mason-Montgomery Road, Mason, OH 45040, USA

Received 6 June 2006; revised 2 August 2006; accepted 3 August 2006

Available online 8 September 2006

Abstract—Utilizing modeling information from a recently resolved structure of human HIF-1 α prolyl hydroxylase (EGLN1) and structure-based design, a novel series of imidazo[1,2-*a*]pyridine derivatives was prepared. The activity of these compounds was determined in a human EGLN1 assay and a limited SAR was developed.
© 2006 Elsevier Ltd. All rights reserved.

Hypoxia inducible factor (HIF) is a transcriptional complex that plays a key role in mammalian oxygen homeostasis and regulates a host of hypoxic response genes that regulate angiogenic, glycolytic, and erythropoietic processes.^{1–3} The subunit components, HIF-1 α and HIF-1 β (ARNT), are constitutively expressed and regulation is achieved by the selective destruction of HIF-1 α . HIF-1 α is a major regulatory point of cellular response to hypoxia (decreasing partial pressure of oxygen).

In the presence of oxygen, a family of three iron-dependent, non-heme prolyl hydroxylases (EGLN-1, EGLN-2, and EGLN-3) effects post post-translational modification of HIF-1 α by hydroxylation of prolines 564 and 402 in the oxygen-dependent degradation domain (ODD) via a reaction that requires 2-oxoglutarate (2OG) and ascorbate.^{4–6} Prolyl hydroxylation then targets HIF-1 α subunits for proteasomal degradation via binding to the VHL (Von Hippel–Landau tumor suppressor protein), elongin C/B, Cullin2, Rbx1 ubiquitin ligase complex.

Since the post-translational hydroxylation of HIF-1 α is strictly dependent on oxygen concentration, under hypoxia the hydroxylation of HIF-1 α is inhibited, and HIF-1 α binds to ARNT to form a functional transcrip-

tional activator that turns on genes with hypoxic response elements (e.g., VEGF, EPO, and glycolytic enzymes).⁷ Therefore, inhibition of HIF-1 α prolyl hydroxylases, resulting in HIF-1 α stabilization, has a potential to be a viable therapeutic approach for ischemic diseases including myocardial infarction, stroke, peripheral vascular disease, heart failure, diabetes, and anemia.

Very limited medicinal chemistry details describing small molecule human HIF-1 α prolyl hydroxylase are reported in the literature.⁸ These inhibitors are small peptidomimetic molecules that resemble 2-oxoglutarate (Fig. 1).

Clearly, there is a strong impetus for the discovery and development of more ‘drug-like’ small molecule HIF-1 α prolyl hydroxylase inhibitors with desirable activity and selectivity profile. In this regard, isoquinoline 3, which acts as a 2-oxoglutarate mimetic and exerts the prolyl hydroxylase inhibition, is a more ‘drug-like’ compound (Fig. 2).⁹ This compound which was discovered

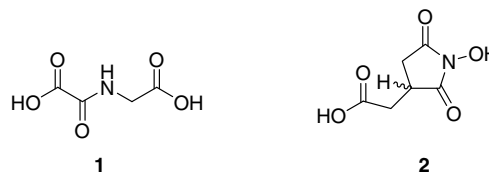


Figure 1. Small molecule HIF-1 α prolyl hydroxylase inhibitors.

Keywords: HIF-1 α prolyl hydroxylase inhibitors; Imidazo[1,2-*a*]pyridines.

* Corresponding author. Tel.: +1 513 622 4467; fax: +1 513 622 0523; e-mail: Warshakoon.nc@pg.com

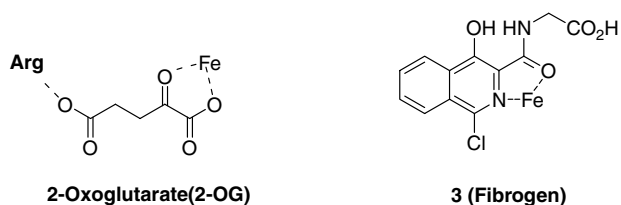


Figure 2. Possible binding modes of 2OG and compound 3.

by scientists at Fibrogen served as the starting point for our medicinal chemistry program on the discovery of HIF-1 α prolyl hydroxylase inhibitors.

We sought to identify new classes of HIF-1 α prolyl hydroxylase inhibitors using structure-based design approach based on the recently solved X-ray crystal structure of EGLN-1 catalytic domain in complex with compound (3) (PDB entry: 2HBT and 2HBU).¹⁰ Our modeling studies (see references and notes section for a detailed description), later confirmed by the X-ray crystal structure, suggested that the isoquinoline nitrogen and the side-chain amide carbonyl interact with iron while the phenolic OH and the amide NH form an intramolecular hydrogen bond which imposes additional rigidity to the molecule (Fig. 3).

Initial modeling studies suggested that imidazo[1,2-*a*]pyridine 4 can be a potential HIF-1 α prolyl hydroxylase inhibitor (Fig. 4). This compound is predicted to interact with the active site in a manner that is different from compound 3: its binding orientation is proposed to be inverted, with the N-1 of imidazo[1,2-*a*]pyridine chelating the iron and the side-chain carboxylate interacting with Arg323 which is located somewhat outside of the active site. By comparison, the side-chain carboxylate of compound 3 interacts with Arg383 which is located inside of the active site (Fig. 3).

Our initial hypothesis based on the initial modeling studies suggested that introduction of substituents on

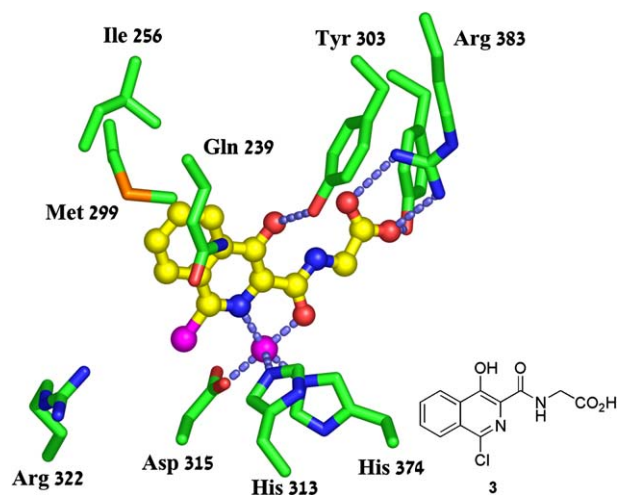


Figure 3. Observed interactions between compound 3 and the enzyme. (Here and in the following figures some residues are omitted for clarity).

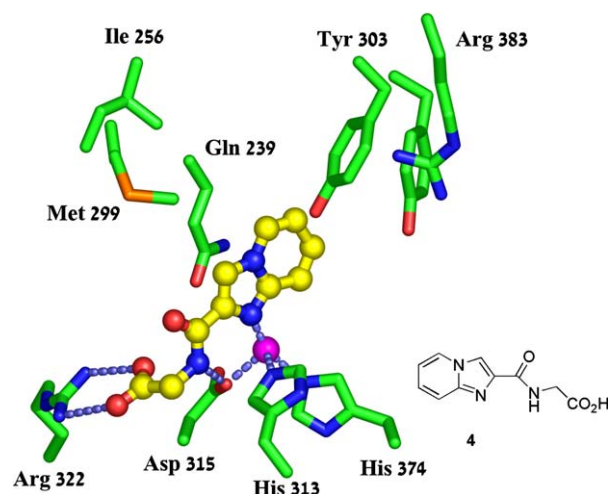


Figure 4. The predicted binding mode of compound 4 in the EGLN-1 active site.

the pyridine ring of the imidazo[1,2-*a*]pyridines would create interactions with the active site toward the Arg383. However, upon examining the binding mode as predicted by FlexX program between 8a and EGLN-1 active site complex, we realized that these compounds bind to the active site in a manner similar to that of compound 3 (Fig. 3) (i.e., the substitution on the pyridine ring now points toward the Arg322 while the side-chain carboxylate interacts with Arg383) (Fig. 5).

Conventionally, the imidazo[1,2-*a*]pyridines can be synthesized via heating a corresponding 2-aminopyridine and bromoglycolate for longer times.¹¹ To rapidly create a library of imidazo[1,2-*a*]pyridines we have decided to employ a new synthetic protocol under microwave conditions.¹² This synthesis generated the desired compounds in excellent yield (80–90%) in 20–30 min. The intermediate 6-bromo imidazo[1,2-*a*]pyridine derivative was hydrolyzed and coupled with glycine methyl ester. This was then subjected to a Suzuki coupling under

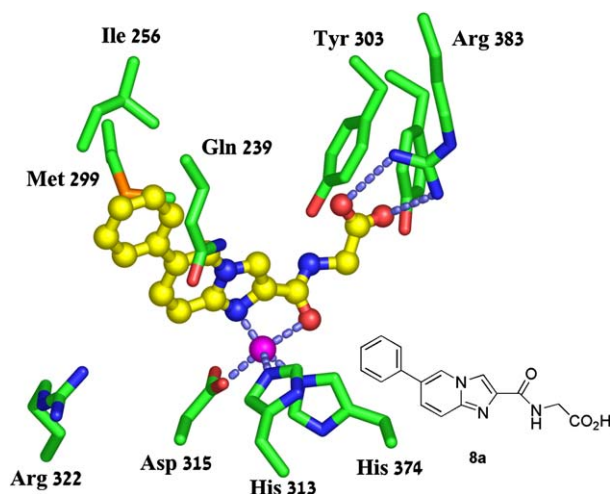


Figure 5. The predicted binding mode of compound 8a in the EGLN-1 active site.

microwave conditions to generate the desired analogs in excellent yields (Scheme 1).

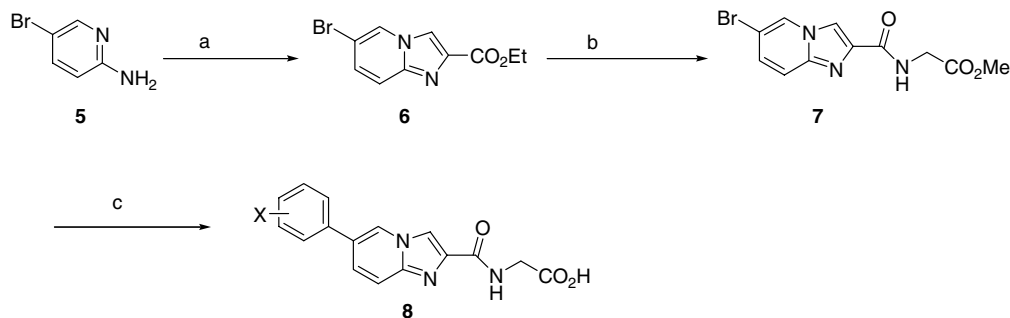
The SAR of the imidazo[1,2-*a*]pyridines is summarized in Table 1. The benchmark isoquinoline **3** had an IC₅₀ value of 1.4 μM in our EGLN-1 assay. Compound **4**, with no substitution on the imidazo[1,2-*a*]pyridine, did not show any activity. Similarly, substitution at 5-, 7-, or 8-position of the imidazo[1,2-*a*]pyridines was completely inactive in EGLN-1 assay. Simple alkyl or halogen substituents at the 6-position of the imidazo[1,2-*a*]pyridines did not show any activity (data not shown). However, introduction of a phenyl group gave appreciable activity. All the compounds with the phenyl ring at the 6-position showed good EGLN-1 activity, with one rare and interesting exception. The methyl substitution at the *meta*-position of the outer phenyl ring (Table 1, **8k**) was completely devoid of any EGLN-1 activity. The *para*-substitution of the outer phenyl ring with both electron-donating and electron-withdrawing groups delivered more active compounds than those of *meta*-substitution. The naphthyl substitution at the 6-position (Table 1, **8h**) generated a compound with good activity toward EGLN-1. Our molecular modeling studies suggest a lipophilic interaction between the naphthyl group and the side chains of Ile256 and Gln239 while the ring nitrogen in the imidazopyridine and the side-chain amide carbonyl coordinate with iron(II) (Fig. 6). In addition, analog **8d** indicates the possibility of generating analogs with superior activity via a simple amide coupling procedure with appropriate amines. In contrast, the analogs derived from 6-amino imidazo[1,2-*a*]pyridines (Table 1, **8m** and **8n**) show a decreasing trend in activity.

In summary, we were able to design and develop a new class of imidazo[1,2-*a*]pyridines based entirely on the crystal structure, that shows promising activity against HIF-1α prolyl hydroxylase. These novel HIF-1α prolyl hydroxylase inhibitors also demonstrated their potential to induce cellular VEGF via stabilizing HIF-1α (data not shown). Analog synthesis and evaluation of physical properties (BA, PK) are currently underway and will be reported in due course.

Modeling studies. The 3D coordinates of receptor was directly adapted from the in-house X-ray structure of human EGLN-1. The 3D structures of compounds to

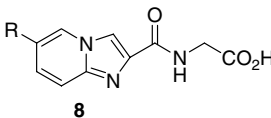
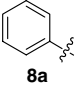
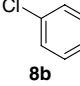
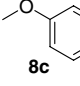
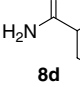
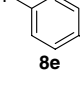
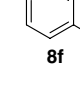
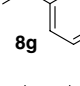
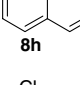
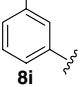
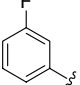
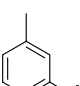
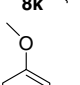
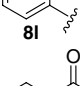
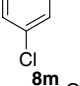
be docked were generated and minimized by Sybyl 7.9 (Sybyl; Tripos Inc., 1699 South Hanley Rd, St. Louis, MO 63144, USA). The protonation state of each compound was assigned based on physiologic condition. For instance, all carboxylic acids were deprotonated. All docking calculations were performed by using FlexX (FlexX; Tripos Inc., 1699 South Hanley Rd, St. Louis, MO 63144, USA) with standard docking procedure and parameters. The active site is defined as the collection of amino acids lying within 6.5 Å of atoms of compound **3** determined by the in-house X-ray structure. FlexX is a fragment-based docking program. The docking conformations were ranked by using FlexX scores. The final protein–ligand complexes were not minimized after the docking. With the same docking set up, we were able to successfully reproduce the binding conformation of compound **3** to EGLN-1. In the predicted protein–ligand complex with the best FlexX score, the rmsd (root mean square deviation) between the coordinates of the predicted ligand and those of the co-crystal ligand is less than 1.5 Å.

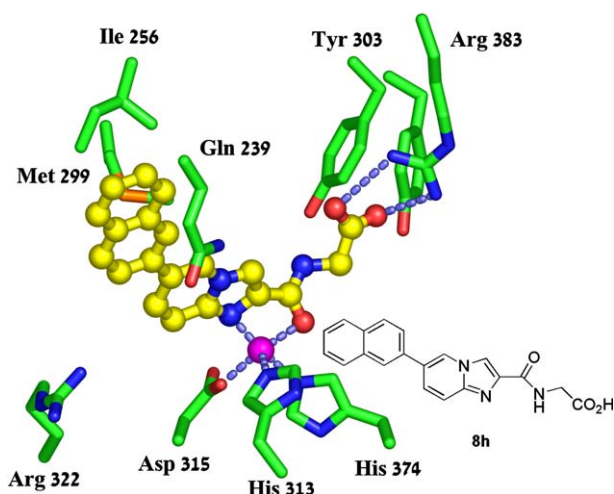
EGLN-1 activity assay. The EGLN-1 enzyme activity was determined using mass spectrometry (matrix-assisted laser desorption ionization, time-of-flight MS, MALDI-TOF MS). The HIF-1α peptide corresponding to residues 556–574 (DLDLEALAPYIPADDDFQL) was used as substrate. The reaction was conducted in a total volume of 50 μL containing Tris–HCl (5 mM, pH 7.5), ascorbate (120 μM), 2-oxoglutarate (3.2 μM), HIF-1α (8.6 μM), and bovine serum albumin (0.01%). EGLN-1, quantity predetermined to hydroxylate 20% of substrate in 20 min, was added to start the reaction. Where inhibitors were used, compounds were prepared in dimethylsulfoxide at 10-fold final assay concentration. After 20 min at room temperature, the reaction was stopped by transferring 10 μL of reaction mixture to 50 μL of a mass spectrometry matrix solution (α-cyano-4-hydroxycinnamic acid, 5 mg/mL in 50% acetonitrile/0.1% TFA, and 5 mM NH₄PO₄). Two microliters of the mixture was spotted onto a MALDI-TOF MS target plate for analysis with an Applied Biosystems (Foster City, CA) 4700 Proteomics Analyzer MALDI-TOF MS equipped with a Nd:YAG laser (355 nm, 3 ns pulse width, 200 Hz repetition rate). Hydroxylated peptide product was identified from substrate by the gain of 16 Da. Data defined as percent conversion of substrate to product was analyzed in GraphPad Prism



Scheme 1. Reagents and conditions: (a) ethyl bromoglycolate/MW/120 °C/20 min; (b) 1—KOH/EtOH/water (90%); 2—HBTU/Gly-OMe/DMF/*i*-Pr₂EtNH (80%); (c) Pd(Ph₃)₄/K₂CO₃/CH₃CN/water/MW/135 °C/15 min (80–85%).

Table 1. Activity of imidazo[1,2-*a*]pyridines against EGLN 1

<div style="text-align: center;">  8 </div>	
R	EGLN1 IC ₅₀ (μM)
	14.2
8a	
	6.8
8b	
	8.1
8c	
	5.9
8d	
	14
8e	
	17
8f	
	16
8g	
	3.6
8h	
	12
8i	
	24
8j	
	>100
8k	
	19
8l	
	24
8m	
	27
8n	

**Figure 6.** The predicted binding mode of compound **8h** in the EGLN-1 active site.

4 to calculate IC₅₀ values (The catalytic domain of EGLN-1 was amplified from a commercially available cDNA from GeneCopia. The vector used is pDONR-221 vector from Invitrogen).

Acknowledgments

N.C.W. wishes to thank Dr. Joseph Gardner for his continuous support and guidance. Ms. Anne Russell and Ms. Marcia Ketcha are gratefully acknowledged for analytical instrumentation support.

References and notes

- Mack, C. A.; Magovern, C. J.; Budenbender, K. T.; Patel, S. R.; Schwatz, E. A.; Zanzonico, P.; Ferris, B.; Sanborn, T.; Isom, O. W.; Crystal, R. G.; Rosengart, T. K. *J. Vasc. Surg.* **1998**, *27*, 699.
- Bruick, R. K.; McKnight, S. L. *Genes Dev.* **2001**, *15*, 2497.
- Safran, M.; Kaelin, W. G., Jr. *J. Clin. Invest.* **2003**, *111*, 779.
- Semenza, G. L. *J. Appl. Physiol.* **2000**, *88*, 1474.
- Semenza, G. L. *Cell* **2001**, *107*, 1.
- Kondo, K.; Kaelin, W. G., Jr. *Exp. Cell. Res.* **2001**, *264*, 117.
- Semenza, G. *Biochem. Pharmacol.* **2002**, *64*, 993.
- McDonough, M. A.; McNeill, L. A.; Tilliet, M.; Papamicaël, C. A.; Chen, Q.-Y.; Benerji, B.; Hewitson, K. S.; Schofield, C. J. *J. Am. Chem. Soc.* **2005**, *127*, 7680; Mole, D. R.; Schlemminger, I.; McNeill, L. A.; Hewitson, K. S.; Pugh, C. W.; Ratcliffe, P. J.; Schofield, C. J. *Bioorg. Med. Chem. Lett.* **2003**, *13*, 2677; Schlemminger, I.; Mole, R.; McNeill, L. A.; Dhanda, A.; Hewitson, K. S.; Tian, Y.-M.; Ratcliffe, P. J.; Pugh, C. W.; Schofield, C. J. *Bioorg. Med. Chem. Lett.* **2003**, *13*, 1451.
- Guenzler, P.; Volkmar, K.; Stephen, J.; Liu, D. Y.; Todd, W. PCT. Int. Appl. WO 2005007192, 2005.
- Evodokimov, *Nat. Struct. Mol. Biol.* **2006**, submitted for publication.
- Kaizerman, J. A.; Gross, M. I.; Ge, Y.; White, S.; Hu, W.; Duan, J.-X.; Eldon, E.; Johnson, K. W. *J. Med. Chem.* **2003**, *46*, 3914.
- Warshakoon, N. C.; Sheville, J.; Gardner, J. H. *Tetrahedron Lett.* **2006**.